



Cite this: *Chem. Commun.*, 2020, 56, 14697

Received 5th September 2020,  
Accepted 3rd November 2020

DOI: 10.1039/d0cc05999d

rsc.li/chemcomm

# Dual H-bond activation of NHC–Au(I)–Cl complexes with amide functionalized side-arms assisted by H-bond donor substrates or acid additives†

Otto Seppänen,<sup>ib ‡a</sup> Santeri Aikonen,<sup>ib ‡a</sup> Mikko Muuronen,<sup>§a</sup> Carla Alamillo-Ferrer,<sup>b</sup> Jordi Burés,<sup>ib b</sup> and Juho Helaja,<sup>ib \*a</sup>

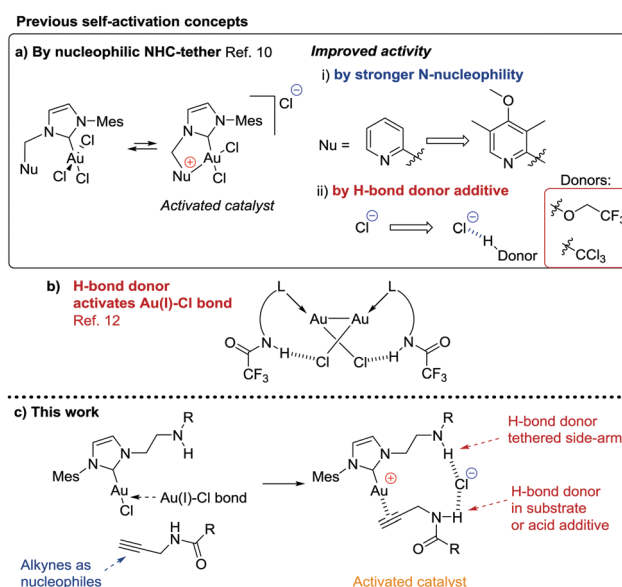
**Novel approach with amide-tethered H-bond donor NHC ligands enabled Au(I)-catalysis via H-bonding. The plain NHC–Au(I)–Cl complex catalysed conversions of terminal N-propynamides to oxazolines, and enyne cycloisomerization with an acid additive, in DCM at RT. DFT calculations enlightened the function of the side-arm in the activation.**

Phosphine and N-heterocyclic carbene (NHC) ligands (L) have brought about adjustable stability, activity, and selectivity for homogeneous gold-catalysed carbon–carbon  $\pi$ -bond activations.<sup>1,2</sup> To access the active cationic gold catalyst from ligated gold–chloride salt (LAuCl), the precatalyst is usually activated with AgX salts by exchanging the Cl<sup>−</sup> counterion to a non- or weakly coordinating one, e.g., BF<sub>4</sub><sup>−</sup>, OTf<sup>−</sup>, NTF<sub>2</sub><sup>−</sup>, PF<sub>6</sub><sup>−</sup>, SbF<sub>6</sub><sup>−</sup>.<sup>3</sup> Many of the activated LAuX catalysts are also commercially available, but these salts are often hygroscopic. *In situ* activation, on the other hand, brings an extra step of removing the precipitate or alternatively carrying out the reaction in the presence of AgCl. The precipitating AgCl residues are non-innocent in gold-catalysis<sup>4</sup> and multiple roles have been assigned for the counter ions.<sup>5,6</sup> Silver-free activations of LAuCl have been reported with sodium salts, e.g., Na[BAR<sup>F</sup><sub>4</sub>],<sup>7</sup> and with strong acid, HBF<sub>4</sub>.<sup>8</sup>

Multifunctional NHC-ligands have shown to be capable to deliver additional designed functions for homogeneous TM catalysis.<sup>9</sup> Recently, ambiphilic ligand Au(I/III) activation strategies have been developed to generate active catalyst without the need of ion exchange. We<sup>10</sup> and others<sup>11</sup> have utilised a pyridine side-arm to replace one chloride ion from the Au(III)

centre with a hemilabile N–Au  $\sigma$ -coordination (Scheme 1a). Additionally, we noted that higher activity was achieved with a more nucleophilic pyridine moiety and in the presence of H-bond donor solvent or additive,<sup>10</sup> which helped to stabilise the cleaved chloride. Previously, Sen and Gabbai integrated the H-bond donor moiety into a phosphine ligand and observed N–H...Cl interactions in the dimer together with aurophilic interaction (Scheme 1b).<sup>12</sup> The dimer equipped with NHCOCF<sub>3</sub> tethered ligand proved to be catalytically active for cyclization of propargylamides, while under same conditions bare PPh<sub>3</sub>AuCl with PhNHCOCF<sub>3</sub> additive was inactive.<sup>12</sup>

Inspired by these findings, we hypothesised that amide-based H-bond donor tethers in NHC ligands would help to activate the Au(I)–Cl bond directly with alkynes *via* N–H...Cl interactions, see Scheme 1c. The approach would circumvent



Scheme 1 Ambiphilic ligand Au-catalyst activation modes.

<sup>a</sup> Department of Chemistry, University of Helsinki, A. I. Virtasen aukio 1, P.O. Box 55, 00014, Finland. E-mail: juho.helaja@helsinki

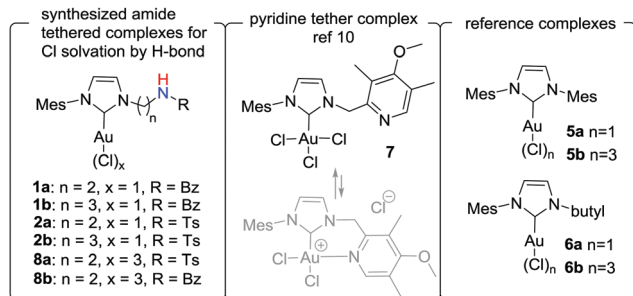
<sup>b</sup> The University of Manchester, School of Chemistry, Oxford Road, M13 9PL Manchester, UK

† Electronic supplementary information (ESI) available. See DOI: 10.1039/d0cc05999d

‡ These authors have equal contributions.

§ M. M. current address: BASF SE, Carl-Bosch-Str. 38, 67056 Ludwigshafen, Germany.





Scheme 2 Studied complexes for catalysis. (Mes = mesityl).

the need to create the vacant site with a hemilabile ligand, thus offering a straightforward approach to activated gold(I)-catalysts.

To probe this hypothesis, we synthesized Au(I) NHC complexes **1a–2b** with benzoyl and tosyl amide tethers bridged with ethyl and propyl linkers (Scheme 2). We selected the cycloisomerization of *N*-(prop-2-yn-1-yl)benzamide **3a** to oxazoline **4a** as a test reaction to investigate the catalytic efficiency due to its popularity in gold catalysis studies.<sup>13</sup>

In catalysts screening (Table 1), the ethyl amide tethered NHC–Au(I) complex **1a** yielded a clean 73% conversion of **3a** to **4a**, while the corresponding tosyl functionalized amide **2a** gave an excellent 95% yield after 3 h monitoring period. Elongating the ethyl arms to propyls lowered the yields to 58% and 67% for Bz (**1b**) and Ts (**2b**) functionalized NHC–Au(I) catalysts, respectively.

The NHC gold complexes without H-bond donors (**5a–6b**) proved to be inactive, while the same complexes gave modest (8%) to decent (68%) yields of **4a** with AgOTs (entries 5–8). Surprisingly, our previously developed self-activated Au(III) complex **7**<sup>10</sup> showed only negligible activity for the reaction, as well as the gold(III)-catalysts **8a** and **8b** (entries 9–11). Although AgOTs or TsOH additives promoted the reaction with **8a** and **8b**, the catalysts were gradually reduced to the respective Au(I)-complexes (see **8b** + TsOH the reaction NMR monitoring in ESI<sup>†</sup>). The solvent screening (Table S2, ESI<sup>†</sup>) exposed that chlorinated solvents CD<sub>2</sub>Cl<sub>2</sub> and CDCl<sub>3</sub> favour the catalysis, while the performance was sluggish in acetone-*d*<sub>6</sub>, CD<sub>3</sub>CN and CD<sub>3</sub>OD.

Table 1 Catalysts screening

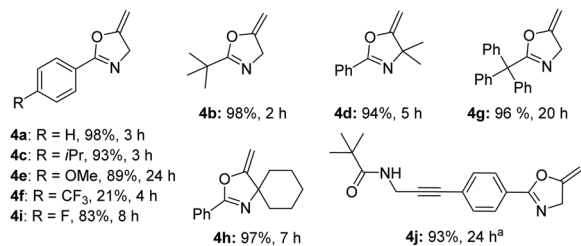
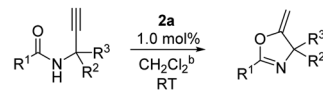
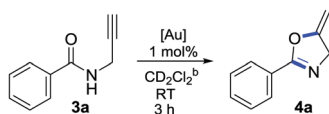
Entry	[Au]	Yield <sup>a</sup> [%] of <b>4a</b>	Entry	[Au]	Yield <sup>a</sup> [%] of <b>4a</b>
1	<b>1a</b>	73	7	<b>6a</b>	0 (68) <sup>c</sup>
2	<b>2a</b>	95	8	<b>6b</b>	0 (30) <sup>c</sup>
3	<b>1b</b>	58	9	<b>7</b>	Trace
4	<b>2b</b>	67	10	<b>8a</b>	20
5	<b>5a</b>	0 (55) <sup>c</sup>	11	<b>8b</b>	5
6	<b>5b</b>	0 (8) <sup>c</sup>	12	IPrAuNTf <sub>2</sub>	58

<sup>a</sup> Determined by <sup>1</sup>H NMR using trimethoxybenzene as internal standard. <sup>b</sup> Water content 150 ppm. <sup>c</sup> With 1 mol% of AgOTs.

Importantly, the complexes **1a–2b** showed comparable or superior activity in comparison to the 58% yield of **4a** with commercially available IPrAuNTf<sub>2</sub> (entry 12). The performance of catalysts **1a–2b** was also better than what has been reported for other NHC or P ligands in homogeneous gold-catalytic conversion with weakly or non-coordinative counter ions (Table S1, ESI<sup>†</sup>).

Next, we studied the substrate scope for the catalytic alkynyl amide oxazoline conversion (Scheme 3) with 1 mol% loading of **2a** in DCM at RT. Several propynamides; <sup>t</sup>Bu (**3b**), electroneutral and rich aryls (**3a, c–e**) provided excellent yields of oxazolines **4a–e**, though an extended reaction time of 24 h was necessary for 4-methoxy-phenyl oxazoline **4e**. Curiously electron deficient 4-CF<sub>3</sub>-phenyl amide (**3f**) provided an unclear reaction and a poor yield of product **4f**, while the 4-F-phenyl oxazoline **4i** was isolated in high 83% yield. Interestingly, bulky functional groups such as triphenylmethyl as R<sup>1</sup> substituent (**4g**) and spirocyclohexyl as R<sup>2</sup> substituent (**4h**) were well tolerated and excellent yields of 96% and 97%, respectively, were received after longer reaction times. Unlike complexes without functional group tethers,<sup>14</sup> the catalyst **2a** proved to be chemoselective towards terminal alkynes as terminally functionalised alkynes **3k** and **3l**, see ESI<sup>†</sup> were unreactive. Similarly, in the case of substrate **3j** that is equipped with both types of alkynes, the terminal alkynylamide cyclised selectively producing **4j** with 93% yield. Additionally, the catalyst was not active for 6-*exo*-dig cyclisation in oxazoline **4m** synthesis (ESI<sup>†</sup>). In the case of terminally substituted alkynes **3j, 3k**, and **3l**, the computational study indicated that steric hindrance between the ligand and the alkynes' terminal substituent limited the reactivity (see Fig. S5, ESI<sup>†</sup>).

The effect of the concentration of water in DCM for the activation of the catalyst (**2a**) became a relevant issue, since aqueous media was previously found necessary for Brønsted acid self-activated ligands (Scheme 1a).<sup>11</sup> We studied the effect of small amounts of water in the solution for the catalytic activity of **2a** in the conversion of **3a** to **4a** in <sup>1</sup>H NMR, see Fig. 1. The results clearly show that even in the absence of water (0 ppm), the catalyst **2a** is activated. The gradual increase of the water content (Fig. 1 and ESI<sup>†</sup>) up to 200 ppm increased the rate and the yield of the reaction, but a higher water content of 250

Scheme 3 Substrate scope in oxazoline synthesis with isolated yields. <sup>a</sup>Catalyst loading 3.0 mol%. <sup>b</sup>Water content in all reactions 150 ppm.

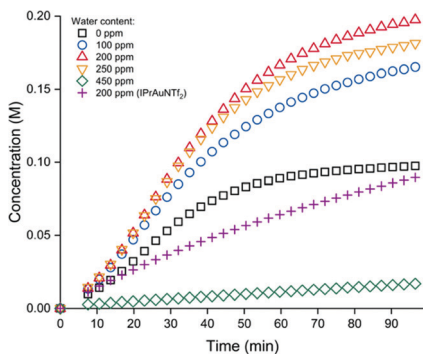


**Fig. 1** Kinetic monitoring of **2a** catalysed conversion of **3a** to **4a** conversion in various water contents. [**3a**] = 0.226 M, and [**2a**]/IPrAuNTf<sub>2</sub>] = 0.0023 M, in CD<sub>2</sub>Cl<sub>2</sub> at 25 °C.

and 450 ppm decreased the rate or even inhibited the reaction, respectively. A plausible explanation for the behaviour is that the small amount of water could assist in the anion solvation (see ESI<sup>†</sup>) or in the proton transfer,<sup>15–17</sup> meanwhile higher amount of water lowers the proton's acidity.<sup>15</sup> An alternative interpretation is that H-bonding interactions between the amide tether and chloride anion are weakened by the water content above 200 ppm thus inhibiting the activation step.

To understand the side-arm's mechanistic role in the Au–Cl bond activation, we compared the computational free energy profiles for catalysts **1a**, **2a**, and **5a** (Fig. 2). Noteworthy, both benzoyl and tosyl amide side-arms lowered the activation free energy barrier in the alkyne addition to the gold, **TS1**, by 2.2 and 3.6 kcal mol<sup>−1</sup>, respectively, compared to **5a** (Fig. 2). The chloride was hydrogen bonded to the side-arm's NH with both **1a** and **2a** while the NH of the substrate coordinated side-arm's sulfonyl oxygen with **2a** (Fig. 2) and the chloride with **1a**. Similar bidentate coordination to chloride in **2a-TS1'** (ESI<sup>†</sup>) was close in energy to **1a-TS1**: 14.0 kcal mol<sup>−1</sup>, whereas the

barrier was 18.2 kcal mol<sup>−1</sup> in the absence of substrate's hydrogen bond coordination in **2a-TS1''** (see ESI<sup>†</sup>).

All catalysts then converged to a tricoordinate complex **B**, from which the chloride spontaneously cleaves (**TS2s** in Fig. 2). The chloride anion hydrogen bonded with NH of the substrate, and with the side-arm's NH if the catalyst was **1a** or **2a** (**Cs** in Fig. 2). The bidentate hydrogen bond donation from the NHs of substrate and side-arm to chloride stabilised **B**, **TS2**, and **C**, over the monodentate hydrogen bonding with **5a** and the stabilisation was stronger with a better H-bond donor, tosyl amide (Fig. 2). Importantly, bidentate H-bonding with **1a** and **2a** favoured the bicoordinate gold-complex over tricoordinate by 1.3 and 2.0 kcal mol<sup>−1</sup>, respectively, whereas the  $\Delta G$  was thermoneutral between **B** and **C** for **5a**.

The rate limiting step of the reaction can either be the C–O bond formation or the protodeauration step for the catalyst **2a**. This will depend on whether the chloride anion is bound to the catalytic complex by hydrogen bonds or solvated by small water cluster. In the former case, the rate-determining step is the protodeauration with 21.3 kcal mol<sup>−1</sup> activation free energy barrier. In the latter case, the rate-determining step is significantly faster with an activation free energy barrier of 17.2 kcal mol<sup>−1</sup> for the C–O bond formation (ESI<sup>†</sup>). This agrees with the observed water effect in Fig. 1. The barriers for **5a** are systematically higher, see ESI<sup>†</sup>.

Beyond the oxazoline synthesis, we investigated how **2a** performed in other classic catalytic L–Au(I) transformations. Echavarren and co-workers have originally reported L–Au(I) catalysed cycloisomerization of enynes (**9** → **10** + **11**, Table 2) and observed no reactivity with bare [PPh<sub>3</sub>AuCl] complex, but exchange of coordinative chloride counterion to SbF<sub>6</sub><sup>−</sup> or BF<sub>4</sub><sup>−</sup> allowed smooth catalytic cycloisomerization at RT.<sup>18</sup> In our case, the enyne **9** was unreactive with 2 mol% loading of **2a** alone (entry 1 in Table 2). However, a 5 mol% addition of mono- and dichloroacetic acid additive gave selectively isomer **10** with

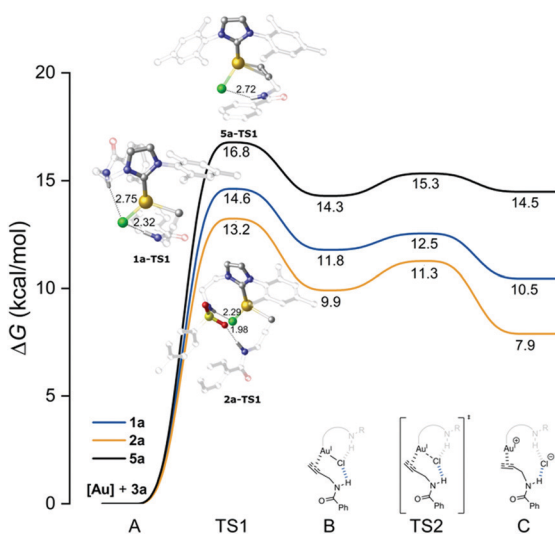


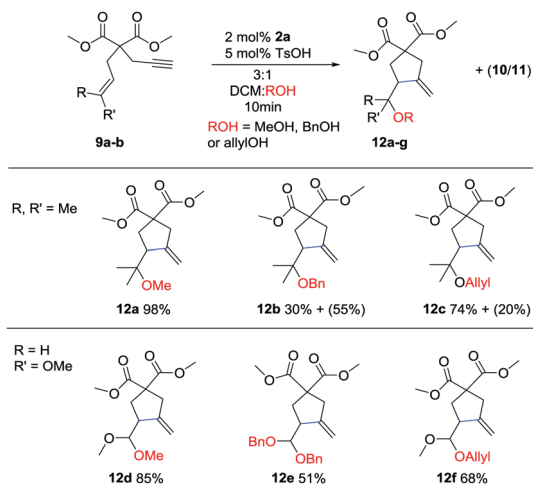
**Fig. 2** Free energy profiles for Au–Cl bond activation with catalysts **1a** (blue line), **2a** (yellow line), and **5a** (black line). Full computational details are in ESI<sup>†</sup>.

**Table 2** Screening of additives for enyne cycloisomerization

Entry	Additive	pK <sub>a</sub> <sup>a</sup>	ΔG(Au–X) <sup>b</sup>	t	Yield <sup>c</sup> <b>10</b> : <b>11</b> (%)
1	—	—	—	1 h	Trace : 0
2	TFE	73.2	—	1 h	Trace : 0
3	AcOH	59.3	−0.5	1 h	Trace : 0
4	ClCH <sub>2</sub> COOH	54.5	4.2	1 h	50 : 0
5	Cl <sub>2</sub> CHCOOH	50.7	7.2	1 h	99 : 0
6	Cl <sub>3</sub> CCOOH	48.4	9.3	40 min	99 : 0
7	TFA	46.2	9.4	15 min	99 : 0
8	MsOH	41.4	12.0	15 min	45 : 54
9	<i>p</i> -TsOH	41.3	14.1	10 min	66 : 33
10	<i>p</i> -TsOH + <b>5a</b>	41.3	14.1	1 h	Trace : 0

<sup>a</sup> Computed pK<sub>a</sub> values in DCM, see ESI for details. <sup>b</sup> Au–X bond strength with the conjugate base relative to Au–Cl in kcal mol<sup>−1</sup>, see ESI for details. <sup>c</sup> Determined by <sup>1</sup>H NMR using trimethoxybenzene as an internal standard.





**Scheme 4** Substrate scope in enyne cycloisomerization, with isolated yields. Yield in parenthesis is the combined yield of products **10** and **11**.

50% and 99% yields, respectively. When TsOH was used as an additive a complete conversion to mixture of isomers **10** and **11** took place in 10 min.<sup>19</sup> The acid additive was unable to activate the non-functionalized complex **5a** in similar efficiency and only traces of product was observed after 1 h (entry 10).

Because chloride's gold-affinity is higher<sup>20</sup> compared to all of the tested acid-additives (Table 2), we reason that the acidity of the additive is important. Inspection of Table 2 reveals that as the acidity of the additive approaches HCl's  $pK_a(\text{DCE}) = 45.2$ ,<sup>21</sup> chloride anion exchange takes place forming an active catalyst for enyne **9** cycloisomerization. Based on the activation mechanism of **2a** in Fig. 2 and in ESI,<sup>†</sup> we reason that the activation of Au–Cl bond with enyne **9** is too high in energy since the enyne substrate has no H-bond donors. Therefore, an acid-additive is needed to help in the activation *via* H-bonding, subsequent protonation and release of HCl, and generation of a loosely coordinating counterion ( $\text{RCO}_2^-$  or  $\text{RSO}_3^-$ ).

The developed acid-assisted activation mechanism was then utilised in enyne cycloisomerization and nucleophilic alcohol (ROH) addition cascade reaction, following previous L-Au(I) catalysis reports (Scheme 4 and Table S3, ESI<sup>†</sup>).<sup>18,22</sup> Full conversion was achieved for each case, and MeOH delivered the best yield of 98% for **12a** while allyl and benzyl alcohols gave lower yields. Similarly, good yields were obtained for OMe-substituted vinyl enyne substrates (**9d–9f**), but benzyl alcohol nucleophile substituted the methoxy group in the product **12e**.

In conclusion, we have developed H-bond donor tethered NHC-ligands for *in situ* activated L-Au(I)Cl catalysis. Ethyl tosyl amide functionalised Au(I) complex **2a** catalysed the oxazole synthesis selectively from terminal alkynes, and successful enyne cycloisomerization was accomplished with an acid additive. Computational analysis supports the dual H-bond donor assisted Au–Cl bond activation mechanism.

Financial support from Academy of Finland [project no. 129062 (J. H.)], Emil Aaltonen foundation [(grant number 180234 (O. S.))] and EPSRC funding [EP/S005315/1 (C. A-F and J. B.)] is acknowledged. The Finnish National Centre for Scientific Computing (CSC) is recognized for computational resources. M. Sc. Karina Moslova is acknowledged for measuring elemental analysis.

## Conflicts of interest

There are no conflicts to declare.

## Notes and references

- D. J. Gorin, B. D. Sherry and F. D. Toste, *Chem. Rev.*, 2008, **108**, 3351.
- W. Wang, G. B. Hammond and B. Xu, *J. Am. Chem. Soc.*, 2012, **134**, 5697.
- M. Jia and M. Bandini, *ACS Catal.*, 2015, **5**, 1638.
- A. Zhdanko and M. E. Maie, *ACS Catal.*, 2015, **5**, 5994.
- (a) M. Jia and M. Bandini, *ACS Catal.*, 2015, **5**, 1638; (b) B. Ranieri, I. Escofeta and A. M. Echavarren, *Org. Biomol. Chem.*, 2015, **13**, 7103; (c) D. Zuccaccia, A. Del Zotto and W. Baratta, *Coord. Chem. Rev.*, 2019, **396**, 103.
- T. Zhou, L. Xu and Y. Xia, *Org. Lett.*, 2013, **15**, 6074.
- M. Wegener, F. Huber, C. Bolli, C. Jenne and S. F. Kirsch, *Chem. – Eur. J.*, 2015, **21**, 1328.
- C. Nevado and A. M. Echavarren, *Chem. – Eur. J.*, 2005, **11**, 3155.
- E. Peris, *Chem. Rev.*, 2018, **118**, 9988.
- (a) M. Muuronen, J. E. Perea-Buceta, M. Nieger, M. Patzschke and J. Helaja, *Organometallics*, 2012, **31**, 4320; (b) M. Muuronen, PhD thesis, University of Helsinki, 2015.
- (a) E. Mendivil-Tomás, P. Y. Toullec, J. Díez, S. Conejero, V. Michelet and V. Cadierno, *Org. Lett.*, 2012, **14**, 2520; (b) E. Tomás-Mendivil, P. Y. Toullec, J. Borge, S. Conejero, V. Michelet and V. Cadierno, *ACS Catal.*, 2013, **3**, 3086.
- S. Sen and F. P. Gabbai, *Chem. Commun.*, 2017, **53**, 13356.
- Key references: (a) A. S. K. Hashmi, J. P. Weyrauch, W. Frey and J. W. Bats, *Org. Lett.*, 2004, **6**, 4391; (b) G. Verniest and A. Padwa, *Org. Lett.*, 2008, **10**, 4379; (c) D. Aguilar, M. Contel, R. Navarro, T. Soler and P. E. Urriolabeitia, *J. Organomet. Chem.*, 2009, **694**, 486; (d) J. P. Weyrauch, A. S. K. Hashmi, A. Schuster, T. Hengst, S. Schetter, A. Littmann, M. Rudolph, M. Hamzic, J. Visus, F. Rominger, W. Frey and J. W. Bats, *Chem. – Eur. J.*, 2010, **16**, 956; (e) O. A. Egorova, H. Seo, Y. Kim, D. Moon, Y. M. Rhee and K. H. Ahn, *Angew. Chem., Int. Ed.*, 2011, **50**, 11446.
- A. S. K. Hashmi, A. M. Schuster, M. Schmuck and F. Rominger, *Eur. J. Org. Chem.*, 2011, 4595.
- R. BabaAhmadi, P. Ghanbari, N. A. Rajabi, A. S. K. Hashmi, B. F. Yates and A. Ariaferd, *Organometallics*, 2015, **34**, 3186.
- M. Chiarucci and M. Bandini, *Beilstein J. Org. Chem.*, 2013, **9**, 2586.
- C. M. Krauter, A. S. K. Hashmi and M. Pernpointner, *Chem Cat Chem*, 2010, **2**, 1226.
- C. Nieto-Oberhuber, M. P. Muñoz, E. Buñuel, C. Nevado, D. J. Cárdenas and A. M. Echavarren, *Angew. Chem., Int. Ed.*, 2004, **43**, 2402.
- Previously, an acid additive ( $\text{HSbF}_6$ ) has been reported to cause similar mixture of isomers in the NHC–Au(I) catalysis: S. Ferrer and A. M. Echavarren, *Organometallics*, 2018, **37**, 781.
- Z. Lu, J. Han, O. E. Okoromoba, N. Shimizu, H. Amii, C. F. Tormena, G. B. Hammond and B. Xu, *Org. Lett.*, 2017, **19**, 5848.
- E. Paenurk, K. Kaupmees, D. Himmel, A. Kütt, I. Kaljurand, I. A. Koppel, I. Krossing and I. Leito, *Chem. Sci.*, 2017, **8**, 6964.
- Y. Tang, I. Benaissa, M. Huynh, L. Vendier, N. Lugan, S. Bastin, P. Belmont, V. César and V. Michelet, *Angew. Chem., Int. Ed.*, 2019, **58**, 7977.

